Civil Engineering Infrastructures Journal, 2026, 59(1): 207-223
DOI: 10.22059/ceij.2025.392043.2273

RESEARCH PAPER

A Comparative Study and Analysis of Transmission Vapor Pipelines for Optimizing Water Purification and Transfer

Aghazadeh, K.[1], Asadzadeh Totonchi, B.[2] and Attarnejad, R.[3*]

[1] Ph.D., School of Civil Engineering, College of Engineering, University of Tehran, Tehran, Iran.
[2] M.Sc., School of Civil Engineering, College of Engineering, University of Tehran, Tehran, Iran.
[3] Associate Professor, School of Civil Engineering, College of Engineering, University of Tehran, Tehran, Iran.

Received: 12 Mar. 2025; Revised: 17 Jun. 2025; Accepted: 28 Sep. 2025

ABSTRACT: Water scarcity poses a significant challenge globally, driving the need for effective solutions in water transport and purification. This paper examines the innovative use of vapor pipelines that leverage water vapor for efficient transportation, based on the principles of evaporation and condensation. It focuses on optimizing water treatment and transmission by investigating pressure differentials that enable vapor flow from the evaporation to the condensation section under sub-atmospheric conditions. The study compares two desalination pipeline systems: an adiabatic system and a steam trap system. Findings indicate that the steam trap system transfers 30% to 35% more water than the adiabatic system, with an additional 5% collected during transit. Temperature assessments reveal that the adiabatic system maintains higher temperatures, correlating with reduced energy consumption, while the steam trap system displays greater variation in vapor velocity. Additionally, the steam trap experiences a 20% greater pressure drop, suggesting potential benefits for the adiabatic approach in specific contexts. Economic feasibility is contingent on environmental conditions, with each system facing distinct operational challenges. This study highlights the necessity of evaluating both systems based on their unique circumstances to effectively tackle the pressing issue of water scarcity. Ultimately, tailored solutions are essential for optimizing water resources worldwide.

Keywords: Water Resource Management; Sustainability; Renewable Energy; Environmental Conservation; Water Science and Technology.

1. Introduction

Water scarcity is a pressing global issue worsened by population growth, urbanization, and environmental decline. As freshwater demand rises, regions face shortages, prompting the need for innovative solutions like seawater desalination, which converts seawater into drinkable water. This paper explores the importance and implications of implementing desalination technologies (Amonovich and Sobir Ahror, 2023; Naeeni et al., 2023; Aghazadeh and Attarnejad, 2026a). Desalination methods such as reverse osmosis and thermal distillation

* Corresponding author E-mail: attarnjd@ut.ac.ir

effectively remove salts and impurities, providing reliable water sources along coastlines. While enhancing drought resilience and diversifying water supplies, these technologies require careful consideration of environmental, economic, and social factors (Rahmani Firozjaei et al. 2024a, 2025; Lotfy et al., 2022).

Environmental challenges include salt discharge impacts, high energy use, and greenhouse gas emissions. Mitigation measures like advanced waste disposal, energy-efficient tech, and renewable energy integration are vital, alongside protecting coastal ecosystems for sustainable desalination (Xue et al., 2020). Economically, desalination demands significant upfront investments, ongoing maintenance, and operational costs. Careful planning, affordable technology, and ensuring equitable access are essential for the technology's long-term success and social acceptance (Al-Mutrafi et al., 2018).

Recent literature converges on three key themes for advancing next-generation desalination: drastically reducing energy consumption through low-temperature or vacuum-assisted processes, integrating renewable energy sources to decarbonize water production, and minimizing or fully recovering brine to protect coastal ecosystems. Membrane-based methods such as forward osmosis and membrane distillation have demonstrated progress at pilot scale, effectively addressing energy reduction and renewable integration, but they still rely on electrically driven circulation pumps and encounter scaling and fouling issues at high salinity levels. Simultaneously, gravity-driven vacuum desalination exploits altitude effects to lower boiling points, yet existing prototypes are typically limited to lengths under 5 km and have not yet addressed the challenge of long-distance water conveyance. Thermal solutions like heat-pipe seawater stills achieve near-adiabatic heat recovery, but the capital costs escalate steeply with increasing pipe diameter beyond a certain threshold, impairing economic viability.

The seawater desalination pipeline system operates efficiently under atmospheric pressure, utilizing minimal thermal energy to evaporate seawater. This innovative system extends from coastal areas to elevated mountainous regions, where significant temperature differences between the warm seawater and the cooler mountain air facilitate the natural movement of water vapor. As the vapor ascends to higher altitudes, it condenses into liquid water, which can then be transported downhill to its intended destination without any additional energy expenditure. This method not only effectively addresses the pressing issue of water scarcity but also leverages natural temperature gradients to optimize overall system efficiency (Aghazadeh and Attarnejad, 2024). Careful consideration of factors like thermal volume optimization and vacuum levels is vital for maximizing desalination performance. Properly designed evaporation and condensation chambers enhance heat exchange and reduce energy losses, enabling sustainable, efficient freshwater production to help alleviate water scarcity (Rahmani Firozjaei et al., 2024b; Sun et al., 2023).

The efficiency of the proposed desalination system is significantly influenced by environmental factors such as temperature fluctuations, altitude, humidity, and atmospheric pressure, all of which affect vapor transmission. Temperature differences between seawater and ambient air drive evaporation and condensation, with higher altitudes improving condensation due to cooler temperatures. Humidity and pressure variations require adaptive controls to maintain stable vapor movement, while seasonal temperature changes are accounted for through simulations to ensure consistent performance year-round. By integrating these environmental considerations, the system is designed to be adaptable and effective across diverse geographic regions facing water scarcity.

Vapor transmission pipelines for desalination offer advantages over conventional methods like reverse osmosis and thermal distillation, such as better energy efficiency using natural temperature gradients, simpler infrastructure with fewer high-pressure pumps, improved water recovery through condensation, and reduced environmental impact. However, its effectiveness depends on local conditions, requiring precise pressure control and specialized engineering. Initial costs and feasibility may be higher, and managing condensation along the pipeline adds complexity. While promising as a sustainable alternative, thorough regional studies are necessary to address operational and environmental challenges.

In vacuum distillation, seawater is heated under reduced pressure, lowering its boiling point to promote evaporation and salt separation. The produced vapor is transported through specialized pipes to a condenser, where it reverts to freshwater. The efficiency of this vapor transport depends on thermal volume, vacuum levels, and the design of the chambers (Ghandi et al., 2025; Grzegorzek et al., 2023; Rahmani Firozjaei et al., 2020).

Vapor transmission pipelines convert liquid water into vapor using pressure and temperature gradients, then condense it back into liquid at the destination. This method offers advantages like lower energy use, less water loss, and reduced costs, but requires careful modeling and optimization of system parameters for maximum efficiency (Hajebi et al., 2024; Hirata et al., 2023). Despite its potential, vapor transfer technology faces challenges in pipeline design, flow management, treatment efficiency, and energy consumption. Robust numerical analysis is essential to address these issues and develop effective water transportation and treatment systems (Bereda et al., 2023; Bonomelli et al., 2024).

The primary objective of this research is to investigate the efficiency and effectiveness of transmission pipelines specifically designed for transporting water vapor during water purification processes. This study focuses on examining two distinct cases concerning the characteristics and operational conditions of the transmission pipeline. In the first scenario, the pipeline is thermally insulated, creating an effectively adiabatic system that prevents heat exchange with the surrounding environment. This configuration is anticipated to enhance the efficiency of the vapor transport process, allowing for the maintenance of optimal temperatures within the system and minimizing energy loss.

In contrast, the second scenario involves a transmission pipeline that lacks thermal insulation, which does not incur additional costs for the creation or maintenance of an adiabatic setup. In this case, heat transfer occurs between the steam and the environment, resulting in the condensation of a portion of the steam within the pipeline.

This research not only aims to deepen the understanding of transmission pipeline dynamics in the context of water vapor transport but also seeks to contribute to the development of best practices for the design and operation of efficient water purification systems. Through a thorough analysis of both insulated and non-insulated scenarios, this study will provide insights into the advantages and trade-offs associated with each configuration, ultimately informing future innovations in vapor transportation technologies in water purification applications. While desalination technologies have traditionally focused on methods such as reverse osmosis and thermal distillation, this study introduces a novel approach by leveraging vapor transmission pipelines to enhance efficiency in water transport. The integration of sub-atmospheric pressure differentials as a driving force for vapor movement represents a fundamental shift in desalination pipeline design, offering significant advantages in energy optimization and system sustainability. By

comparing adiabatic and steam trap configurations, this research provides new insights into the interplay between thermal insulation, pressure management, and water yield, addressing critical gaps in previous studies. The findings not only contribute to advancing desalination infrastructure but also pave the way for scalable, energy-conscious solutions in global water resource management.

2. Methodology

The overall design of the desalination pipeline system is illustrated in Figure 1. The system is divided into three primary components: the evaporation section, the transportation section, and the condensation section.

i) Evaporation section: This segment collects seawater, wastewater, or rainwater, de-aerated, evaporates, and transforms into vapor under sub-atmospheric pressure in a heated environment. Before evaporation, it is crucial to remove soluble gases such as carbon dioxide and oxygen from the seawater. These gases, which cannot be condensed, remain in the transportation pipeline, potentially leading to increased pressure within the system.

ii) Transportation section: In this section, the steam produced during the evaporation phase must be transported to its destination via transfer pipes. The temperature difference between the evaporation and condensation sections creates a pressure differential, facilitating the flow of steam from the evaporation section to the condensation section. This segment ensures that the steam produced in the evaporation phase is adequately prepared for transfer. The vapor, being cooler than the ambient temperature, requires additional heat to maintain process continuity and efficiency. As a result, the steam heats up as it flows through the warmer transfer section towards the condenser. In the horizontal transfer zone, condensation is minimal due to the temperature being close to that of the surrounding environment. However, as the height of the transfer increases, the temperature drop of the steam within the pipe accelerates, while the surrounding environment's temperature decreases more rapidly due to elevation.

At this stage, two scenarios for the pipeline are defined, which are the focus of this research. The first scenario posits that the transmission pipeline is insulated thermally, making the transfer system effectively adiabatic with no heat exchange with the environment. In this scenario, the water vapor in the pipe experiences only temperature differences resulting from friction, compressibility, or changes in height, preventing any phase change, and thus maintaining a single-phase flow throughout the transfer process.

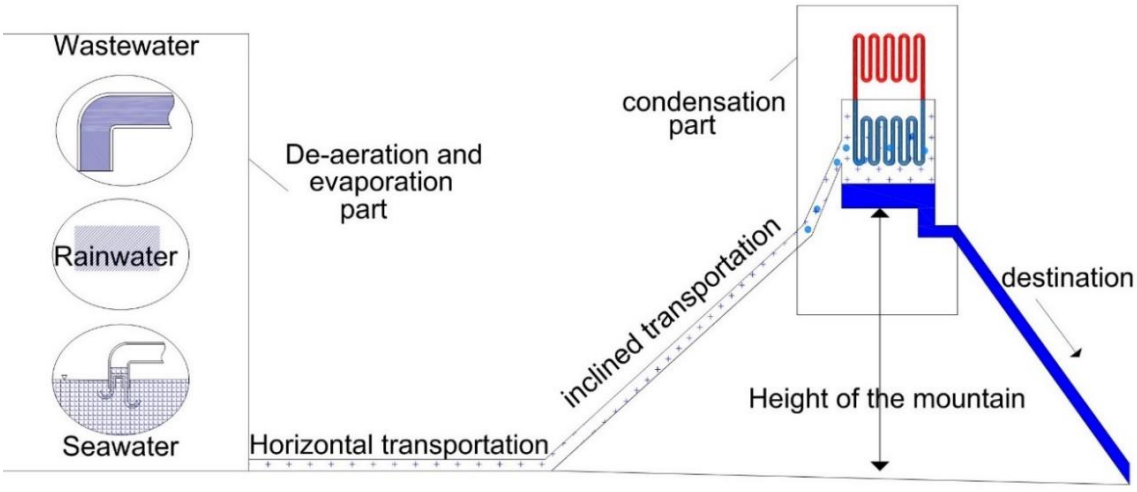

Fig. 1. Schematic outline of the desalination pipeline system

In the second scenario, the system is not thermally insulated, and no additional costs are incurred for creating or maintaining an adiabatic system. Consequently, heat transfer to the environment leads to the condensation of a portion of the steam within the transmission pipe. As condensation occurs, the heat extracted from the steam is transferred to the pipe walls, maintaining their temperature in equilibrium with the water vapor. With only water vapor present in the system, the pressure inside the pipe aligns with the pressure corresponding to the ambient temperature, indicating a stable equilibrium. This equilibrium demonstrates that the vapor tends to remain saturated. The system actively works to maintain this stability against any disturbances. If the pressure rises or the temperature decreases, additional vapor condenses to restore equilibrium and reduce the internal pressure. Conversely, if the pressure drops or the temperature increases, the vapor enters a non-saturated state, which increases internal pressure. The system compensates for this by evaporating liquid water within the pipe, thereby stabilizing the operating temperature across all components.

This approach simplifies operational conditions and reduces overall costs. Condensed water, which may form as a result of this process, should be collected in a designated chamber, relying on gravity for this purpose. To prevent the risk of system procedure from the 2-phase flow, the collecting of water is essential. For this reason, steam traps are strategically installed under the transportation pipe. Collecting the condensed water helps maintain a vacuum condition within the system. When valves are opened, external pressure prevents the complete drainage of water from the pipe, with the volume of drained water approximately equal to that at altitudes exceeding 10 m. Supported steam traps are employed to facilitate the transfer of condensed water into an adjacent pipe for continued operation, ensuring the system remains efficient and effective during the condensation process (Aghazadeh and Attarnejad, 2025).

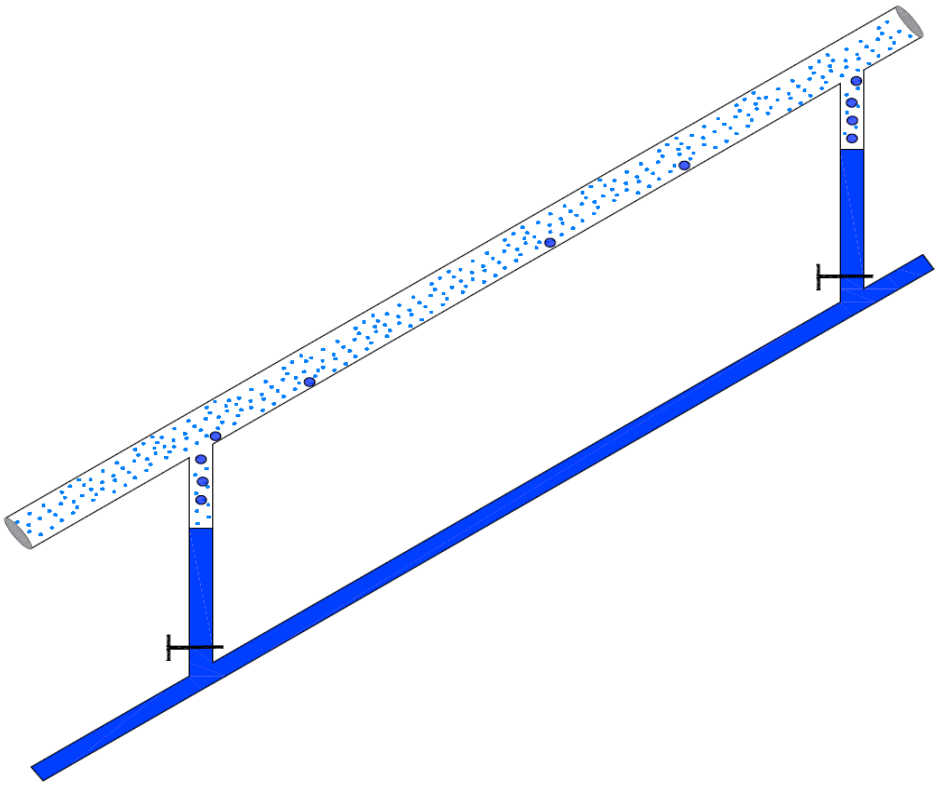

Fig. 2. Schematic representation of the removal of condensed water by steam traps

iii) Condensation section: In this final stage, the steam that has passed through the transportation section is converted back into liquid water. Various methods can be employed for this conversion, including condensation chambers, heat pipes, and phase-change energy-prompted Processes. However, this research focuses exclusively on the transportation aspect and does not delve into the details of the condensation stage. The process concludes with the preparation of potable water through the addition of essential minerals, ensuring compliance with established consumption standards. This comprehensive design effectively harnesses the principles of thermodynamics and fluid mechanics to convert seawater into potable water efficiently. It also addresses critical operational factors, including pressure differentials and energy recovery, enhancing overall system performance.

The overall calculation framework is based on several key assumptions to streamline the analysis. It assumes that steam behaves according to the ideal gas law due to low-pressure conditions throughout the system. The pipeline's horizontal sections are maintained at ambient temperature, with minor condensation effects considered negligible, while at higher altitudes, water is immediately collected to ensure flow remains single-phase. The surrounding air temperature is assumed to vary linearly with altitude, reflecting natural environmental gradients. All parameters are treated as constant over time, adhering to steady-state conditions to simplify the analysis. Detailed dynamics of evaporation and condensation, such as pressure drops during phase changes, are omitted to focus on transportation processes.

Throughout the system, sub-atmospheric pressure is maintained to facilitate vapor movement, and the latent heat of vaporization is assumed to be stored within the evaporation section for energy balance. The entire pipeline system is designed to be fully sealed to prevent water ingress, ensuring system integrity. Additionally, the initial transportation pipeline is considered adiabatic, meaning no heat exchange occurs with the environment during transit. Finally, the pipes are modeled as round, smooth, and resistant to flow resistance, which helps optimize efficiency and reduce energy losses.

3. Formulation

This section explores the flow equations that govern steam transfer within a pipeline. A representative segment of the pipe is considered, and the relevant equations are formulated accordingly. In shorter pipes and nozzles, the effects of viscosity can generally be neglected; however, for longer pipelines, it is essential to account for flow friction against the pipe walls. To facilitate practical formulation, a finite volume element of the pipe is selected, from which the governing equations for fluid transfer are derived based on the principles of continuity, energy, and momentum. The results of this formulation apply comprehensively to the entire length of the transfer system.

A thorough understanding of the physical aspects of the problem is paramount. Key parameters include the linear distance, the elevation difference between the cold and warm points, and the range of temperature variations between these points. The pipeline may consist of numerous interconnected segments, each exhibiting distinct thermodynamic conditions at the inlet and outlet, which leads to variable fluid velocities across the segments. Figure 3 illustrates the pipeline at various positions with a constant diameter, exemplifying a transport pipeline. To accurately analyze the behavior of the pipeline, three fundamental equations (continuity, momentum, and energy) are utilized to calculate the velocity and temperature at the pipe outlet, specifically at the moment when the steam reaches the condensation stage.

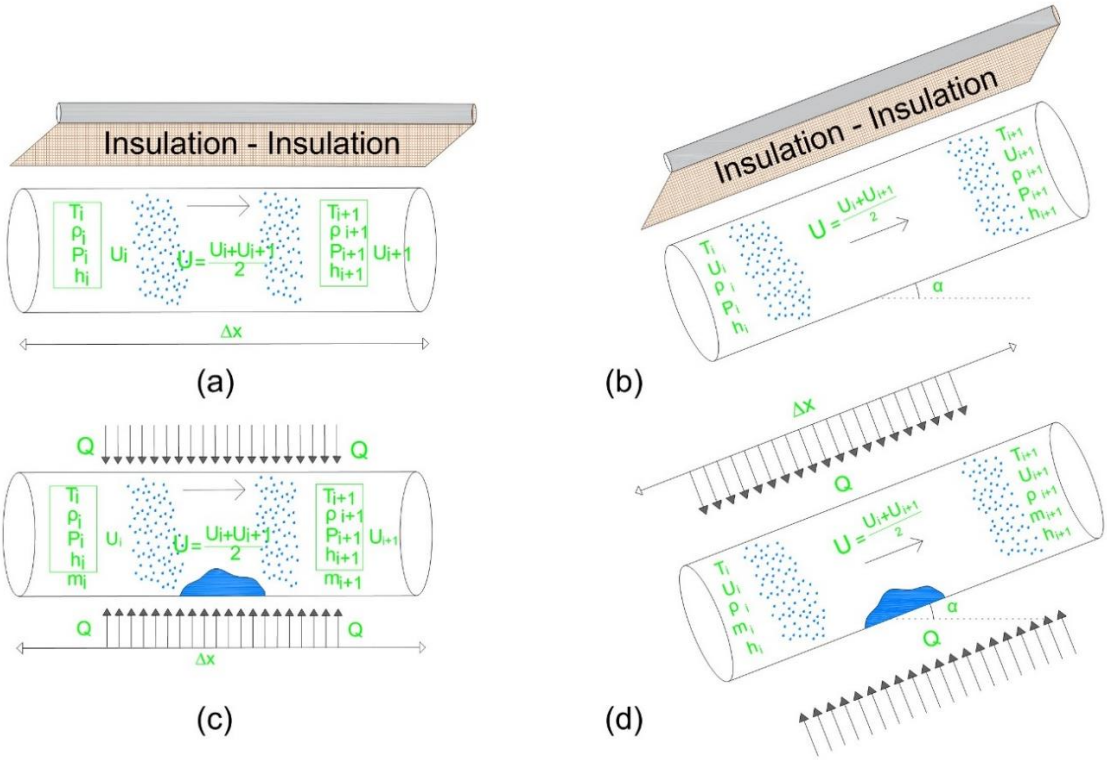

Fig. 3. A typical element of the: a) Horizontal adiabatic transfer pipeline; b) Inclined adiabatic transfer pipeline; c) horizontal transfer pipeline equipped with steam trap; and d) Inclined transfer pipeline equipped with steam trap

Continuity equation as Eq. (1) (Gas Processors Suppliers Association, 2004; Anderson, 1983):

$$\frac{\partial \rho}{\partial t} + \frac{\partial (\rho U)}{\partial x} = 0 \qquad (1)$$

where ρ: is the density of water vapor (kg/m^3), u: is the vapor's velocity (m/s) and t: is the time.

Momentum equation as Eq. (2):

$$-\frac{\partial (\rho U^2)}{\partial x} - \frac{\partial P}{\partial x} - \frac{4}{D}\tau_w - \rho g sin(\alpha) = \frac{\partial (\rho U)}{\partial t} \qquad (2)$$

where ρ, U, P, D, τ_W, g, and α represent vapor density, vapor velocity, vapor pressure, pipe diameter, wall shear stress, gravitational acceleration, and the angle of pipeline relative to the horizon, respectively.

Energy equation as Eq. (3) according to the first law of thermodynamics.

$$\triangle U = \frac{dE}{dt} = Q - W = 0 \qquad (3)$$

where $\triangle U$: is the change in internal energy of the system, Q: is the heat added to the system and W: is the work done by the system.

In the first scenario, where the transmission pipeline is equipped with thermal insulation and does not exchange heat with the environment, the main governing equations can be simplified to Eqs. (4-5) (Attarnejad and Aghazadeh 2020).

$$\rho_i u_i = \rho_{i+1} u_{i+1} \qquad (4)$$

$$p_i - p_{i+1} = \rho g \Delta z + \rho_{i+1} {u_{i+1}}^2 - \rho_i {u_I}^2 + \frac{2fL\rho U^2}{D} \qquad (5)$$

where p: is the vapor pressure (Pa), g: is the acceleration due to gravity (m/s^2) and Δz: is the height difference between the two ends of the element (m).

Eq. (6) can be written according to the first law of thermodynamics (Aghazadeh

and Attarnejad, 2026b).

$$\left(h_i + \frac{{u_i}^2}{2} + g\Delta z\right) - \left(h_{i+1} + \frac{{u_{i+1}}^2}{2}\right) = 0 \quad (6)$$

where *h*: is the vapor enthalpy (J/kg) and Δx: denotes the length of the element.

Simultaneously, when solving the governing equations, variations in density, velocity, temperature, and pressure along the transport pipeline can be determined. The mass flow rate through the pipe can be calculated through a comprehensive analysis of the transport pipeline and the extraction of relevant parameters as Eq. (7).

$$m_t = \rho_i \frac{\pi D^2}{4} u_i \quad (7)$$

where m_t: is the transportation rate (kg/s) and *D*: is the pipe diameter (m).

In the second scenario, where the system lacks thermal insulation and employs a steam trap to collect vapors, Eqs. (1) to (3) can also be rewritten and simplified as follows (Aghazadeh and Attarnejad, 2020). Based on the continuity equation, it is understood that the rate of vapor transport yields a singular result for each element, thus diminishing the necessity to write out the equations for each variable individually as Eqs. (8-9).

$$\rho_i u_i A = \rho_{i+1} u_{i+1} A + (m_i - m_{i+1}) \quad (8)$$

$$\mathrm{Q}.\Delta x + (m_i - m_{i+1}) h_{fg} - m_i \left(h_i + \frac{{u_i}^2}{2} g\Delta z\right) m_{i+1} \left(h_{i+1} + \frac{{u_{i+1}}^2}{2}\right) = 0 \quad (9)$$

where *h*: is the vapor enthalpy (J/kg), *Q*: is the amount of heat flow extracted per unit length (W/m), Δx: is the length of the element and h_{fg}: is the change of specific enthalpy from saturated vapor into saturated liquid and it is negative value due to condensation (J/kg).

In order to obtain the heat exiting the pipe, Eq. (10) is used in the transition phase (VDI-Gesellschaft Energietechnik, 1992):

$$Q = \frac{T_I - T_o}{\frac{R_I}{2\pi r_1} + \frac{ln(\frac{r_2}{r_1})}{2\pi\lambda_k} + \frac{R_o}{2\pi r_2}} \quad (10)$$

where T_I: is the temperature of the liquid inside the pipe (K), T_o: is the external air temperature (K), R_I: is the inner surface heat transfer resistance between fluid and material of the pipe ($\mathrm{m}^2.\mathrm{k/w}$), R_o: is the outer surface heat transfer resistance between fluid and material of the pipe ($\mathrm{m}^2.\mathrm{k/w}$), λ_k: is the thermal conductivity of pipe (W/m.K), r_1: is the internal radius of the pipe (m), and r_2: is the external radius of the pipe (m).

To calculate the pressure difference along each segment of the pipeline, Eq. (11) is applied, incorporating hydrostatic, frictional, and dynamic effects.

$$p_i - p_{i+1} = \rho g \Delta z + \frac{2fL\rho U^2}{D} + \rho_{i+1} {u_{i+1}}^2 - \rho_i {u_I}^2 \quad (11)$$

where *f*: is friction coefficient, *L*: is segment length (m) and *U*: is the median velocity of vapor (m/s).

After analyzing the transfer pipe and obtaining the speed, temperature and other necessary parameters for each element, the amount of mass transmitted through the pipe is calculated as Eq. (12).

$$m_{t1} = \rho_n \frac{\pi D^2}{4} u_n \quad (12)$$

where m_{t1}: is the rate of vapor that has been transferred and should be condensed (kg/s) and *D*: is the pipe diameter (m).

After analyzing the transport pipeline and obtaining the velocity, temperature, and other requisite parameters for each element, the mass transmitted through the pipe can be expressed mathematically. To ascertain the total amount of condensed water along

the pipeline, it suffices to aggregate the condensed water amount from each element as Eq. (13).

$$m_{t2} = \sum_{i=1}^{n} m_i \quad (13)$$

where m_i: is the condensation rate in ith element (kg/s), n: is the number of elements and m_{t2}: is the condensation rate in the transport part (kg/s).

To quantify the behaviour of water-vapour flow in both the adiabatic and steam-trap pipelines, a one–dimensional, steady-state model that couples mass, momentum, and energy conservation was developed and solved in Python.

4. Case Study

This system is applicable to various locations near high altitudes, particularly regarding seawater. However, this research specifically targets the seawater of the Persian Gulf in Iran, with a case study focused on Bandar Abbas City. Bandar Abbas is a notable coastal city situated along the Persian Gulf, serving as the capital of Hormozgan Province. It functions as a crucial commercial and transportation hub, boasting strategic port facilities. The city is recognized for its vibrant culture and rich history. Located northwest of Bandar Abbas is Genu Mountain, which rises to an altitude of 2,347 m. This cooler mountainous area offers a stark contrast to the warm coastal climate of Bandar Abbas. Genu Mountain is celebrated for its natural beauty and biodiversity, attracting outdoor enthusiasts and researchers interested in studying the ecological and meteorological differences between coastal and mountainous regions.

The case study involves collecting meteorological data to analyze the climate interactions between Bandar Abbas and Genu Mountain. This includes the mean sea temperature of Bandar Abbas, the city's air temperature, and ambient temperatures at various elevations of Genu Mountain, all detailed in Figure 4. The horizontal distance between the Persian Gulf and Genu Mountain is approximately 15.5 km, consisting of segments measuring 2.5 km, 2 km, and 11.5 km, in addition to the horizontal distance there is the inclined distance. The inclined distance is about 11.5 km which is different from horizontal distance. Average temperatures in Bandar Abbas and ambient temperatures at Genu Mountain's elevations are illustrated in Figure 4. Additionally, the geographical relationships between the Persian Gulf, Bandar Abbas City, and Genu Mountain are depicted in Figure 5.

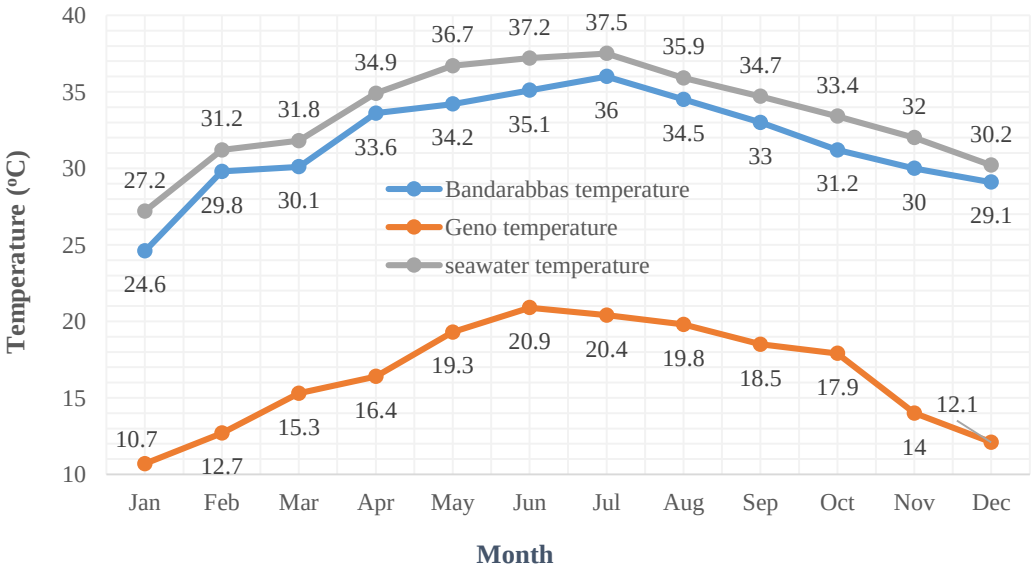

Fig. 4. Air temperature and seawater temperature for target regions

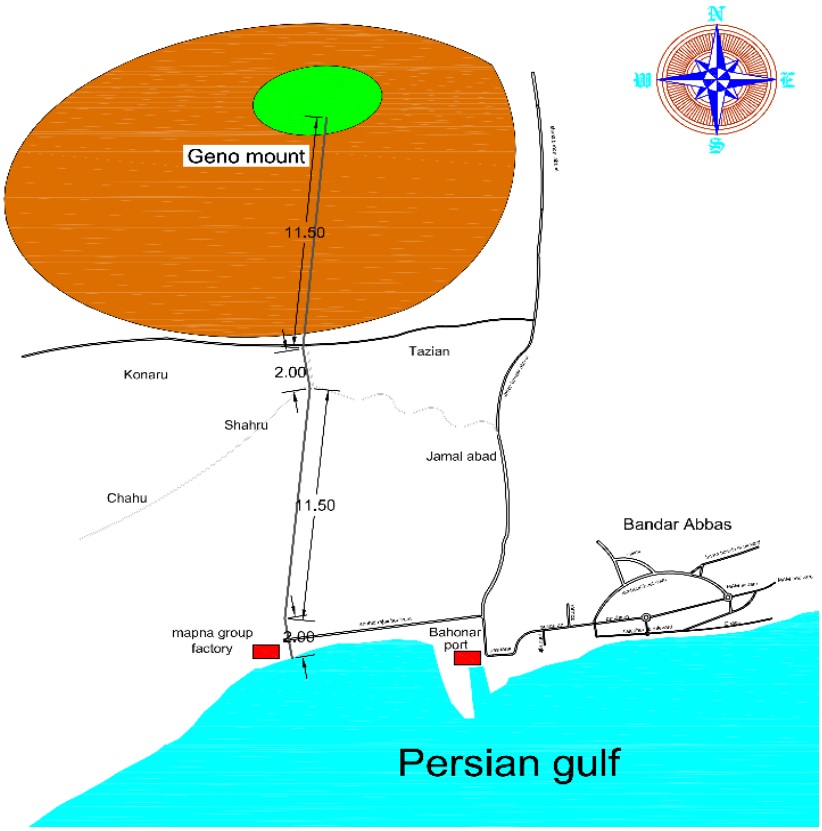

Fig. 5. Location of coastal Bandarabbas city and Genu Mountain

5. Results and Discussions

5.1. Calculation Method

In the proposed desalination pipeline system, it is assumed that evaporation and condensation rates always exceed the transfer rate, making transfer the limiting factor in the process. Therefore, the analysis focuses solely on the transfer rate and compares results between the first and second scenarios. To balance computational efficiency and accuracy, a spatial step of 100 m has been chosen based on previous experience with solving transportation equations numerically. Before starting calculations, it is important to identify key factors such as the temperatures of the warm source, cold source, and environment, as these influence thermal dynamics. The length of the horizontal pipeline must be specified, while the inclined section's length and height are also critical. The pipeline's arrangement, including the segments and their intervals, should be clearly defined; each segment will be set at 100 m to ensure consistency and accuracy in the modeling process.

Once these foundational parameters have been established, the next phase involves calculating key fluid properties at the end of each element within the horizontal pipeline. This includes determining the temperature, density, pressure, and velocity of the fluid, using transportation equations tailored to these specific conditions. These calculations will be repeated for all elements along the pipeline until the endpoint is reached. Moreover, it is essential to calculate the maximum transportation rate within this section (first scenario ($m_{t.horizental}$), second scenario ($m_{t1.horizental}$), along with the exit temperature ($T_{e.horizental}$), and to evaluate the behavior of any condensed vapor present within the pipeline (m_{t2}).

Following the completion of the horizontal pipeline calculations, a similar approach is applied to the inclined pipeline. The same fluid properties like temperature, density, pressure, and velocity must be calculated using the earlier determined exit

temperature ($T_{e.horizental}$), from the horizontal section, along with other relevant information. These computations will provide insight into the performance of the inclined segment, allowing for the determination of the maximum transportation rate ($m_{t.inclined}$), and the temperature at the inclined section's peak.

At this stage, it is vital to derive key values resulting from the calculations. Specifically, the temperature at the top of the mountain section (T_e) must be closely defined, and the overall transportation rate (m_t) will be set as the minimum between the rates obtained from the horizontal and inclined pipelines. Finally, a comprehensive assessment of the evaporation and condensation processes will be conducted in accordance with the calculated transportation rates, along with other essential parameters, to ensure a thorough understanding of the system's thermal dynamics. This structured approach enables a systematic examination of the transportation pipeline, facilitating accurate predictions and assessments of the fluid behavior under varying conditions.

5.2. Calculation Results for the System in Target Regions: Adiabatic Transportation Pipeline and Transportation Pipeline with Steam Trap

Using the available data, including temperature, height, length, and diameter of the selected transmission pipe, the transmission capacity is calculated based on the equations derived in the previous section. These transmission capacity calculations are implemented in a Python program. Since the transmission capacity serves as the limiting factor for this system, the results obtained from both scenarios are compared.

Figure 6 presents the quantities of produced and transferred water, along with the temperature at the end of the pipe, measured at 1 m and 2 m for this system operating with adiabatic pipes. According to our findings, the volume of distilled and transported water for a 1-m diameter transmission pipe is calculated to be 26,595 m^3/year, while for a 2-m diameter pipe, it is 124,830 m^3/year.

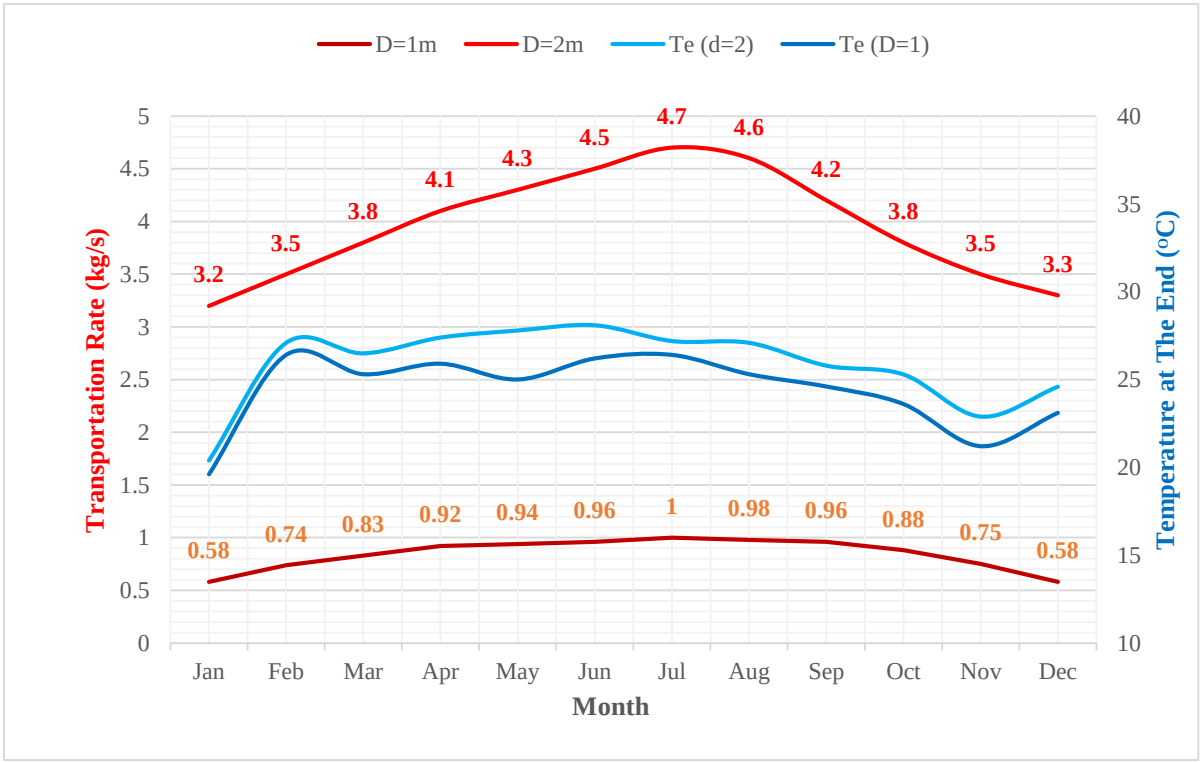

Fig. 6. Distilled and transferred water and vapor temperature at end of the pipe in the first scenario

Figure 7 illustrates the steam velocity within the transmission pipe as well as the corresponding pressure drop in the system for pipe diameters of 1 m and 2 m, specifically in the context of adiabatic pipes. A lower pressure drop within the system indicates an enhanced capacity for the length of transportation pipe. As shown in Figure 6, an increase in pressure drop correlates with elevated temperatures at the end of the pipe. This is significant because a higher temperature in the end of the transmission pipe results in an increased temperature of the water vapor during condensation, ultimately leading to reduced energy requirements for the condensation process.

In the case of the transmission pipe with a diameter of 1 m, a greater pressure drop was observed compared to that of the 2 m diameter pipe. Despite the minimal difference in velocity between the two pipes, this variation in pressure drop can be attributed to the smaller diameter of the 1 m pipe, which experiences a more pronounced effect of friction. Consequently, the frictional losses in the narrower pipe are more impactful, resulting in a lower pressure drop and improved transmission efficiency.

At this stage, the results pertain to the second scenario, in which the thermal insulation of the pipe is compromised, resulting in a non-adiabatic system. In this scenario, the changes in steam conditions are taken into account due to condensation occurring within the water pipe. Consequently, it is essential to report not only the volume of water transferred through the system but also the amounts of water that are generated during the transportation process. This analysis highlights the significance of accounting for the water collected due to condensation, as it contributes to the overall efficiency and productivity of the system. By evaluating both the transferred and produced water quantities, a comprehensive understanding of the system's performance can be gained under non-adiabatic conditions.

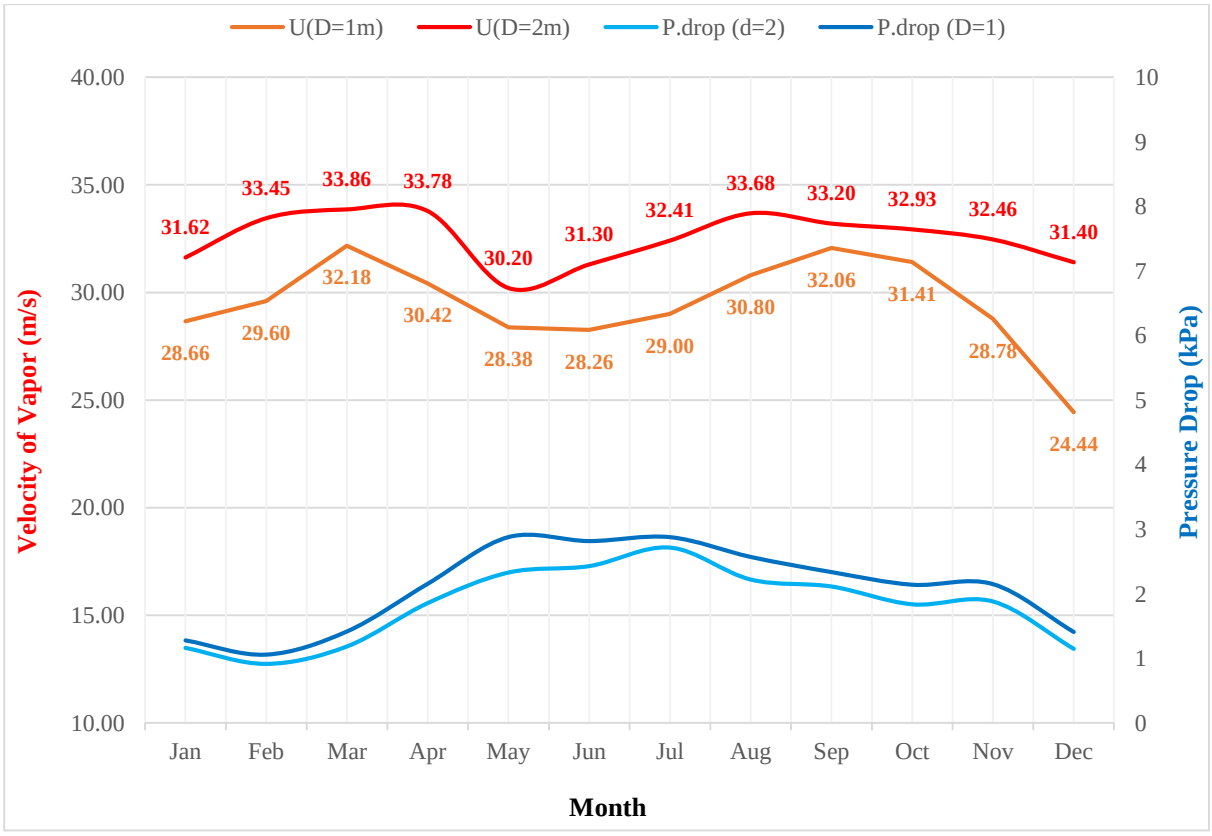

Fig. 7. Vapor speed and system pressure drop in the first scenario

Figures 8 and 9 depict the volume of water produced in the area, along with the length of the transportation route and the destination. These figures also provide information on the temperature at the end of the pipe and the vapor velocity within the transportation pipe, with reference to the pipe diameter, either 1 m or 2 m. For a 2 m diameter pipe, the production rate of distilled water at the destination is 165,301 m^3/year. In contrast, the production rate for a 1 m diameter pipe is significantly lower, at 35,478 m^3/year. Additionally, the volume of water produced during the transportation phase, given the specified pipe diameters, is 8,751 m^3/year for the 2 m diameter pipe and 2,024 m^3/year for the 1 m diameter pipe. The capacities of both pipe diameters indicate that the water production is consistent with the flow rate of a small aqueduct. The calculations demonstrate that the desalination pipeline system is capable of supplying distilled water annually. However, it is essential to note that the production rate of refined water is positively influenced by the temperature differential between the seawater and the air temperature on land.

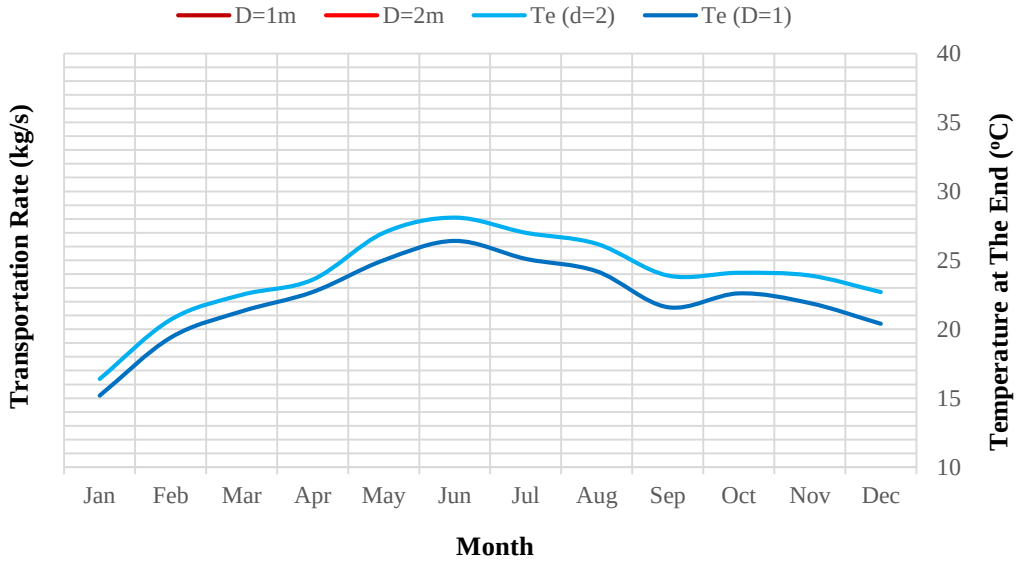

Fig. 8. Distilled and transferred water and vapor temperature at end of the pipe in the second scenario

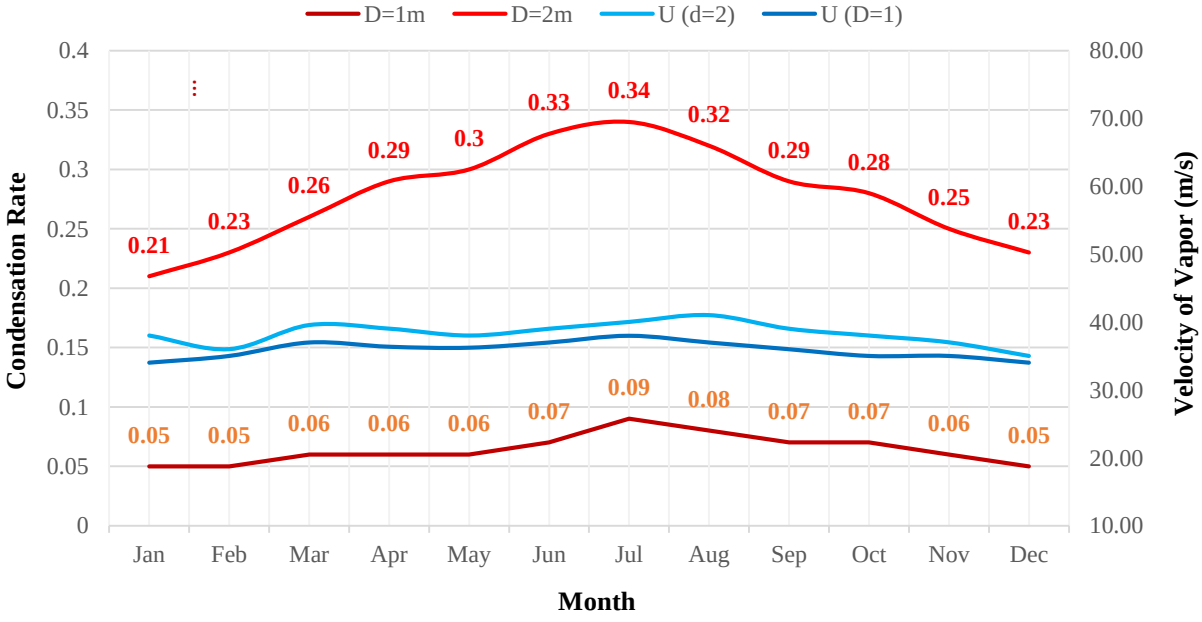

Fig. 9. Monthly production rate of distilled water in transportation part, m_{t2} and vapor speed in the second scenario

Figure 10 illustrates the pressure drop within the system for pipe diameters of 1 m and 2 m, specifically in the context of adiabatic pipes. The results demonstrate a pattern similar to that observed in the first scenario; however, the values associated with the pressure drop are notably higher than those in the previous conditions. This indicates that the system exhibits greater transmission capability over longer distances in the initial scenario. As with the previous findings, the 1 m diameter pipe exhibits a more pressure drop compared to the 2 m diameter pipe. Despite the minimal difference in steam velocity between the two pipes, the increased pressure drop in the 1 m pipe can be attributed to its smaller diameter, which leads to a more pronounced effect of friction. Consequently, the frictional losses in the narrower pipe are more significant, resulting in a greater pressure drop and influencing the overall efficiency of the transmission system.

Based on the results presented above, the differences between the two states of transmission pipeline system are evident. This study examines two scenarios: the first scenario represents an adiabatic system, while the second scenario involves steam traps. The findings indicate that the volume of water transferred in the second scenario was greater than in the first scenario, with variations observed across different months due to changing conditions. Specifically, the amount of water transferred in the second scenario ranged from 30% to 35% more than that in the first scenario. Additionally, there was an extra 5% of mentioned water along the route in the second scenario.

Temperature measurements reveal that the average temperature at the end of the pipe and the vapor entering the condensation phase differ between the two scenarios. For the first scenario, the average temperatures for the 1 m and 2 m diameters were 25.85 °C and 24.38 °C, respectively. In contrast, the second scenario recorded temperatures of 22.15 °C and 23.85 °C for the same diameters. Higher temperatures at the end of the pipe correlate with reduced energy consumption during the condensation phase. Moreover, elevated steam temperatures under consistent conditions indicate greater steam power for continued transmission. The results above can be verified using the references introduced in the introduction, which include both numerical and experimental studies. This combination enhances reliability by integrating theoretical modeling with empirical validation.

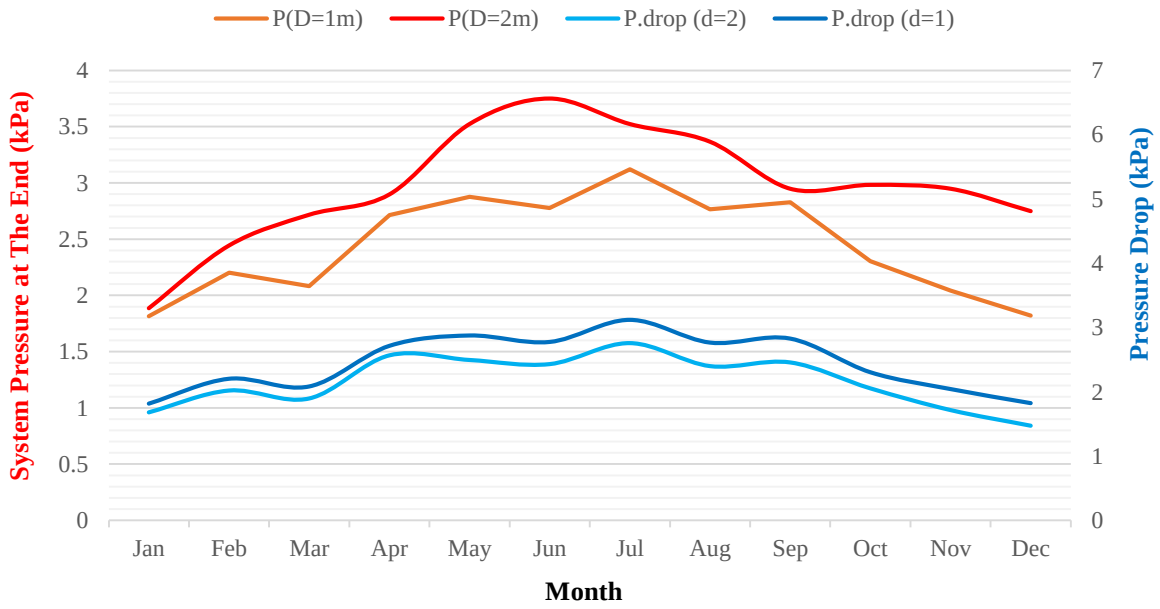

Fig. 10. Vapor pressure at destination and system pressure drop in the second scenario

A more detailed analysis was conducted to confirm the statistical robustness of the observed 30-35% increase in water transfer with the steam trap system. Using a Monte Carlo uncertainty analysis, random realizations for each pipeline diameter (1 m and 2 m) and scenario (adiabatic vs. steam trap), was generated based on published data. The resulting annual transferred volume distributions, summarized by their means and 95% confidence intervals, indicate a statistically significant mean increase of approximately 33% for the 1 m diameter and 31% for the 2 m diameter.

Vapor velocity was similar in both scenarios, but speed variations were more pronounced in the second due to lower end-pipe temperatures. The pressure drop was 20% higher in the second scenario, favoring the adiabatic system for longer steam travel. Environmental factors impact feasibility, adiabatic systems require insulation, while steam-trap systems need high-altitude piping and space. Each system has distinct advantages, requiring evaluation based on specific conditions.

A Levelized-Cost-Of-Water (LCOW) model analyzed two pipeline layouts over 25 years at a 6% discount rate, considering CAPEX (capital expenditure for construction and installation), routine O&M (annual operations and maintenance costs), and energy costs (2025 USD). The adiabatic system requires insulation costing 150 USD/m, adding 6 M USD to a 40 km route, while the steam-trap system avoids insulation but requires traps at 7 USD/m, totaling 0.28 M USD. Annual O&M for steam traps is 85000 USD, compared to 40000 USD for the insulated line, and energy costs are 19000 USD/year for steam-trap fans, while the adiabatic system requires none. Despite higher O&M and energy costs, the steam-trap system achieves a five-fold lower LCOW due to dramatically reduced CAPEX and greater volumetric yield. Even at 0.35 USD/kWh or double maintenance costs, LCOW remains below the adiabatic system.

6. Conclusions

This study investigated the differences between two states of a transmission pipeline system used in desalination: an adiabatic system and a system utilizing steam traps. For ease of comparison, the two configurations were discussed case-by-case. In the fully adiabatic line (Scenario A) a 1 m diameter pipe delivered about 26,600 m^3 of distilled water per year, while enlarging the pipe to 2 m raised output to roughly 124,800 m^3. The higher end-of-line vapor temperatures (≈ 25.9 °C for 1 m and 24.4 °C for 2 m) cut condensation-stage energy use, and the overall pressure drop was about 20 % lower than in the alternative design. Capital expenditure, however, was elevated because continuous thermal insulation was required. Conversely, the non-insulated line equipped with steam traps (Scenario B) achieved larger throughputs, approximately 35,500 m^3/year for a 1 m pipe and 165,300 m^3/year for a 2 m pipe, plus an additional 5% condensate recovered along the route. These gains came at the cost of a steeper pressure gradient (≈ 20% higher) and slightly greater condensation energy because the vapor reached the condenser colder (≈ 22.1 °C and 23.9 °C, respectively). Although the omission of insulation trims initial capital outlay, routine maintenance of the steam-trap network must be factored into long-term operating costs. In practice, regions with pronounced temperature gradients and where volumetric yield is paramount favor the steam-trap design; energy-constrained sites or those with modest ΔT and expensive elevation works are better served by the adiabatic alternative.

7. Declaration

Artificial intelligence (AI) tools were only used to enhance the grammar, clarity, and professional presentation of the manuscript. No AI methods were employed in the research, data analysis, or modeling presented in this study.

8. References

Aghazadeh, K. and Attarnejad, R. (2026a). "High-pressure desalination pipeline system for water purification and vapor transfer utilizing waste heat from factories", *Applied Water Science*, 16, 101, https://doi.org/10.1007/s13201-026-02795-0.

Aghazadeh, K., Asadzadeh Totonchi, B. and Attarnejad, R. (2026b). "Energy-efficient water reuse system for high-rise buildings utilizing sub-atmospheric pressure and temperature gradients", *Urban Water Journal*, 2026(Mar 6),1-8, https://doi.org/10.1080/1573062X.2026.2639445.

Aghazadeh, K. and Attarnejad, R. (2025). "Experimental investigation of friction coefficient in water vapor transportation pipelines under sub-atmospheric pressure", *European Journal of Mechanics, B/Fluids*, 2025 (Nov 1), 114, https://doi.org/10.1016/j.euromechflu.2025.204319.

Aghazadeh, K. and Attarnejad, R. (2024). "Experimental investigation of desalination pipeline system and vapor transportation by temperature difference under sub-atmospheric pressure", *Journal of Water Process Engineering*, 60(March), 105133. doi:10.1016/j.jwpe.2024.105133.

Al-Mutrafi, H., Al-Zubari, W., El-Sadek, A. and Abdel Gelil, I. (2018). "Assessment of the water-energy nexus in the municipal water sector in Eastern Province, Saudi Arabia", *Computational Water, Energy, and Environmental Engineering*, 07(01), 1-26, https://doi.org/10.4236/cweee.2018.71001.

Amonovich, M.R. and Niyozov, S.S.A. (2023). "Importance of water for living organisms and national economy, physical and chemicl methods of wastewater treatment", *American Journal of Research in Humanities and Social Science*, 9(1), 7-13, https://americanjournal.org/index.php/ajrhss/article/view/387.

Anderson, J.D.J. (1983). "Modern compressible flow", *International Journal of Heat and Fluid Flow* 4(1), 59-60, https://doi.org/10.1016/0142-727X(83)90029-2.

Attarnejad, R. and Aghazadeh, K. (2020). "Study of sweetened seawater transportation by temperature difference", *Heliyon* 6(3), e03573, https://doi.org/10.1016/j.heliyon.2020.e03573.

Bereda, Y.B., Tesfamariam, B.B., Desissa, T.D., Habtamu, G., Singh, B. and Ramulu, P.J. (2023). "Utilization of silica-enriched filter cake industry by-products as partial ordinary portland cement replacement", *Materials Research Express*, 10(2), 025502, https://doi.org/10.1088/2053-1591/acaf4d.

Bonomelli, R., Pilotti, M. and Heidarian, P. (2024). "DEBRA: A multi-rheological 2D steep shallow water finite volume scheme for debris flow propagation in mountain areas", *EGU General Assembly 2024 (EGU24)*, Vienna, Austria, 14-19 Apr., Abstract EGU24-4141, https://doi.org/10.5194/EGUSPHERE-EGU24-4141.

Ghandi, E., Mohammadi Rana, N. and Esmaeili Niari, S.H. (2025). "Parametric analysis of axially loaded partially concrete-filled cold-formed elliptical columns subjected to lateral impact load", *Civil Engineering Infrastructures Journal*, 58(1), 49-70, https://doi.org/10.22059/ceij.2024.364758.1955

Gas Processors Suppliers Association (GPSA). (2004). *GPSA engineering data book*, 11th Edition, Tulsa, OK, USA: Gas Processors Suppliers Association.

Hajebi, Z., Rahmani Firozjaei, M., Naeeni, S.T.O. and Akbari, H. (2024). "Hydraulic performance of bottom intake velocity caps using PIV and OpenFOAM methods", *Applied Water Science*, 14(3), 1-13, https://doi.org/10.1007/s13201-023-02091-1.

Hirata, Y., Kawai, K., Kato, T., Fujimoto, H., Tameno, Y., Ishikawa, T., Matsuoka, H., Akasaka, H. and Ohtake, N. (2023). "Characterization of structural and mechanical properties of DLC films deposited on the surface of minute-scale 3D objects: Comparison of PECVD and FCVA deposition technique", *Surface and Coatings Technology*, 460, 129401, https://doi.org/10.1016/j.surfcoat.2023.129401.

Lotfy, H.R., Staš, J. and Roubík, H. (2022). "Renewable energy powered membrane desalination, Review of recent development", *Environmental Science and Pollution Research*, 29(31), 46552–46568, https://doi.org/10.1007/s11356-022-20480-y.

Grzegorzek, M., Wartalska, K. and Kaźmierczak, B. (2023). "Review of water treatment methods with a focus on energy consumption", *International Communications in Heat and Mass Transfer*, 143, 106674, https://doi.org/10.1016/j.icheatmasstransfer.2023.106674.

Naeeni, S.T.O., Rahmani Firozjaei, M., Hajebi, Z. and Akbari, H. (2023). "Investigation of the performance of the response surface method to optimize the simulations of hydraulic phenomena." *Innovative Infrastructure Solutions*, 8(1), 10, https://doi.org/10.1007/s41062-022-00977-8.

Rahmani Firozjaei, M., Behnamtalab, E. and Salehi Neyshabouri, S.A.A. (2020). "Numerical simulation of the lateral pipe intake: Flow and sediment field", *Water and Environment Journal*, 34(2), 291-304, https://doi.org/10.1111/wej.12462.

Rahmani Firozjaei, M., Naeeni, S.T.O. and Akbari, H. (2024a). "Evaluation of seawater intake discharge coefficient using laboratory experiments and machine learning techniques", *Ships and Offshore Structures*, 19(9), 1394-1407, https://doi.org/10.1080/17445302.2023.2247125.

Rahmani Firozjaei, M., Hajebi, Z., Naeeni, S.T.O. and Akbari, H. (2024b). "Discharge performance of a submerged seawater intake in unsteady flows: Combination of physical models and decision tree algorithms." *Journal of Water Process Engineering*, 60, 105198, https://doi.org/10.1016/J.JWPE.2024.105198.

Rahmani Firozjaei, M., Hajebi, Z., Naeeni, S.T.O., Akbari, H. and Iglesias, G. (2025). "Hydrodynamic performance of seawater intake structures through numerical modelling and particle image velocimetry", *Water*, 17(17), 2607, https://doi.org/10.3390/w17172607.

Sun, H., Wang, S., Sun, L., Ling, Z. and Zhang, L. (2023). "A novel low-temperature evaporation wastewater treatment apparatus based on hydrate adsorption", *Review of Scientific Instruments*, 94(9), 094101, https://doi.org/10.1063/5.0161972.

VDI-Gesellschaft Energietechnik. (1992). *Engineering reference book on Energy and heat*. VDI Verlag.

Xue, W.J., Cui, Y.H., Liu, Z.Q., Yang, S.Q., Li, J.Y. and Guo, X.L. (2020). "Treatment of landfill leachate nanofiltration concentrate after ultrafiltration by electrochemically assisted heat activation of peroxydisulfate", *Separation and Purification Technology*, 231, 115928, https://doi.org/10.1016/j.seppur.2019.115928.

9. Nomenclature

D	Diameter of pipe (m)
h	Enthalpy of vapor (J/kg)
L	Length of the element
M	Mass flow rate of wastewater (kg/s)
m_t	Rate of evaporation (kg/s)
m_{t1}	Rate of transportation (kg/s)
m_{t2}	Rate of condensation vapor (kg/s)
p_s	Pressure of the system (kPa)
Q	Amount of heat flow extracted per unit length (W/m)
Q_c	Total heat used in the condensation part
t	Time
T_e	Temperature at the end of the pipe (°C)
T_s	Temperature of the system (°C)
u	Vapor velocity (m/s).
w	Work input (W/m)
Δz	Height of the element (m)
τ_w	Wall shear stress (N/m^2)
λ_c	Latent heat of condensation of vapor (J/kg)
λ_e	Latent heat of vaporization of water (J/kg)
ρ	Density of vapor (kg/m^3)